Contribution from the Laboratoire de Chimie de Coordination du CNRS, 31030 Toulouse-Cedex, France, and Department of Chemistry, University of Michigan, Ann Arbor, Michigan 48109

Microwave Spectrum and Nitrogen-14 Nuclear Electric Quadrupole Coupling Constants in *cis*-Thionylimide and Iminosulfur Oxydifluoride: Orientation and Analysis of the Electric Field Gradients

PATRICK CASSOUX,*[1a] ALAIN SERAFINI,[1a] GERALD FONG,[1b] and ROBERT L. KUCZKOWSKI*[1b]

Received July 21, 1977

The ^{14}N nuclear quadrupole coupling constants for $DNSOF_2$ have been measured. They are $\chi_{aa} = 2.44 \pm 0.25$ MHz, $\chi_{bb} = -0.67 \pm 0.85$ MHz, and $\chi_{cc} = -1.77 \pm 0.67$ MHz. These data, when combined with previous measurements for $HNSOF_2$, HNSO, and DNSO, give the orientation and magnitudes of the principal axes of the electric field gradients in both compounds. Notable differences in the magnitudes are observed. The orientation of electric field gradient tensor in the molecular symmetry planes are respectively for $HNSOF_2$ and HNSO about 17 and 26° from the N–S bond direction. The electronic structure of the two compounds has also been analyzed by ab initio MO–SCF calculations. The agreement with experiment for the relative signs, magnitudes, and orientation of the computed electric field gradient tensor is very satisfactory. The calculations also indicated that the major source of the differences in the quadrupole coupling constants can be attributed to increased electron density in the nitrogen p orbital perpendicular to the symmetry plane in $HNSOF_2$ and increased π-bonding character in the nitrogen–sulfur bond.

Introduction

The microwave spectra of *cis*-HNSO and *trans*-$HNSOF_2$[2] have been recently analyzed.[4,5] The structures and dipole moments were reported along with the ^{14}N quadrupole coupling constants for HNSO, DNSO, and $HNSOF_2$. It is interesting to note that upon addition of two fluorines to HNSO, the most prominent structural changes are a significant shortening of the N–S bond distance and a reorientation of the hydrogen from cis to trans. In going to $HNSOF_2$ there is also a large increase in the dipole moment and a sign reversal for the out-of-plane quadrupole coupling constant (χ_{cc}), which is by symmetry a principal axis of the field gradient tensor in both molecules. The large change in χ_{cc} was especially puzzling since the coupling constant is determined largely by the charge density near the nitrogen nucleus and both species nominally have the same hybridization about nitrogen and nearly identical HNS bond angles. It was suggested in ref 5 that the change could be indicative of increased electron density in the nitrogen p_π orbital and increased π character in the N–S bond in $HNSOF_2$.

In order to understand better the origin of the differences between HNSO and $HNSOF_2$, an investigation of their electronic structures has been made by ab initio MO–SCF calculations. Also, the microwave spectrum of $DNSOF_2$ was investigated to obtain the ^{14}N quadrupole coupling constants. The inertial axes of $HNSOF_2$ rotate about 23° upon deuteration. Therefore, the associated large change in χ_{aa} and χ_{bb} permits a determination of the orientation of the principal axes of the electric field gradient tensor and the magnitude of these field gradients. A similar analysis was performed for HNSO using literature results.[4] These experimental values for the field gradients and their orientations could also be compared against the theoretical values.

Experimental Section

Sample. The sample of $HNSOF_2$ described in ref 5 was deuterated by several exchange cycles with D_2O. The enrichment was about 60%.

Spectrometers. The conventional 80-kHz Stark modulated spectrometer and a Hewlett-Packard 8460A spectrometer with 33-kHz modulation described in the previous study were used.[5] The cell was cooled with dry ice. Frequencies were reproducible to ±0.05 MHz. However, true line centers may be in error by slightly more due to experimental difficulties from overlapping Stark effects, incomplete resolution due to the small hyperfine splittings, and proximity to perturbing strong Q branch lines of $HNSOF_2$ or $DNSOF_2$.

$DNSOF_2$ Spectra. The rotational constants and a number of pressure broadened transition frequencies for $DNSOF_2$ have been previously reported.[5] Nearly every predicted R branch, *b* dipole transition up to $J = 3 \rightarrow 4$ for $DNSOF_2$ was examined for splittings; unfortunately, many of the strong transitions had splittings too small for measurement.

Table I. Calculated and Observed ^{14}N Quadrupole Hyperfine Structure for $DNSOF_2$ in MHz[e]

$J \rightarrow J'$	ν_0(pred)[a]	ν_0(obsd)[b]	$F \rightarrow F'$	ν_F(obsd)	$\Delta\nu_F$[c]
1_{11}–2_{02}	18 244.32	18 244.30 ± 0.03	0 → 1	18 243.30	0.04
			1 → 2	18 245.11	−0.02
			2 → 3	18 244.10	−0.02
1_{01}–2_{12}	18 675.17	18 675.16 ± 0.07	0 → 1	18 675.91	0.03
			1 → 2	18 674.93	0.05
			2 → 3	18 675.23	−0.07
2_{21}–3_{12}	27 263.17	27 262.96 ± 0.01	1 → 2	27 262.2[d]	−0.08
			2 → 3	27 263.89	0.00
			3 → 4	27 262.68	0.00
2_{12}–3_{03}	27 500.84	27 500.94 ± 0.08	1 → 2	27 500.91	−0.04
			2 → 3	27 501.09	0.06
			3 → 4	27 500.91	−0.06
3_{22}–4_{13}	36 732.10	36 732.01 ± 0.12	2 → 3	36 731.95[d]	0.21
			3 → 4	36 732.31	0.09
			4 → 5	36 731.95	−0.08
3_{30}–4_{23}	35 262.45	35 262.40 ± 0.03	2 → 3	*d*	
			3 → 4	35 263.39	−0.03
			4 → 5	35 262.08	0.02
3_{31}–4_{22}	35 934.70	35 934.70	4 → 5	35 934.39	−0.01
			2 → 3	*d*	
			3 → 4	*d*	

[a] Predicted using *A*, *B*, and *C* in ref 5. [b] Average hypothetical unsplit center frequency calculated from observed ν_F's and derived coupling constants. [c] $\Delta\nu_F = \nu_F$(obsd) − ν_F(calcd). [d] Difficult to measure; not used in determining χ_{aa} and η. [e] ^{14}N quadrupole coupling constants derived from splittings: $\chi_{aa} = 2.44 \pm 0.25$, $(\chi_{bb} - \chi_{cc})/\chi_{aa} = 0.455 \pm 0.31$.

The transitions reported in Table I could be resolved at sample pressures of about 3–10 mTorr and the quadrupole coupling constants determined from them by a least-squares fitting method employing all the data. The procedure consisted of fitting the splittings to $eQq_a = \chi_{aa}$ and $eQq_a\eta = \chi_{bb} - \chi_{cc}$ using equations 6-1 and 6-19 in ref 6 and quantities calculated from our asymmetric rotor program. This gave the coupling constants (χ_{aa}, η) and the hypothetical unsplit frequencies (ν_0) listed in Table I. The uncertainties in χ_{aa} and η were estimated from the relationships $\Delta\chi_{aa}/\Delta\nu \approx \Delta\eta/\Delta\nu \approx 5$ obtained from these equations. The agreement is considered satisfactory, although not as good as for $HNSOF_2$[5] where much better line shapes could be obtained.

Because η is small, the splittings were not sensitive to it. This limits the accuracy of χ_{bb} and χ_{cc} which can be obtained: $\chi_{bb} = -0.67 \pm 0.85$, $\chi_{cc} = -1.77 \pm 0.67$ MHz. The value for χ_{cc} can be compared with the result for $HNSOF_2$ where it is -2.21 ± 0.01 MHz.

Quadrupole Principal Axis Field Gradients. Upon isotopic substitution, the inertial principal axes of a molecule rotate causing changes

0020-1669/78/1317-1204$01.00/0

Table II. Nitrogen-14 Nuclear Quadrupole Coupling Constants in Principal Axes System of the Quadrupole Tensor Determined from Experiment and ab Initio MO Calculation

Molecule	Method	θ_{xa}[a]/deg	χ_{xx}/MHz	χ_{yy}/MHz	χ_{zz}/MHz
$HNSOF_2$	Exptl	37.5 ± 1.1	−1.38 ± 0.01	3.59 ± 0.32	−2.21 ± 0.01
	Ab initio	40.86	−1.20	3.79	−2.60
HNSO	Exptl	36.4 ± 4.0	−3.21 ± 0.50	1.64 ± 0.75	1.57 ± 0.14
	Ab initio	39.29	−3.09	1.61	1.48

[a] Angle between quadrupole tensor x axis and inertial a axis. See Figures 1 and 2 for the orientation of the in plane x and y axes.

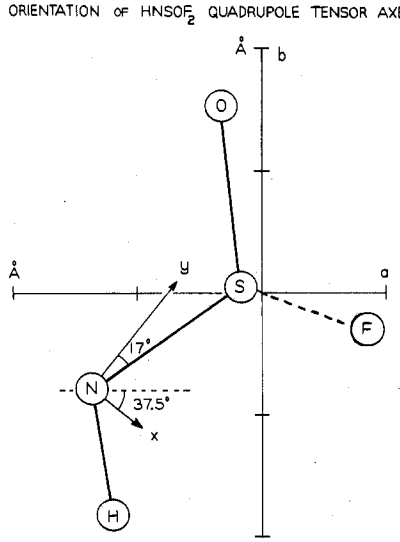

Figure 1. Projection of $HNSOF_2$ in symmetry plane showing principal inertial axes (a, b frame) and principal field gradient axes (x, y frame) of the nitrogen nucleus.

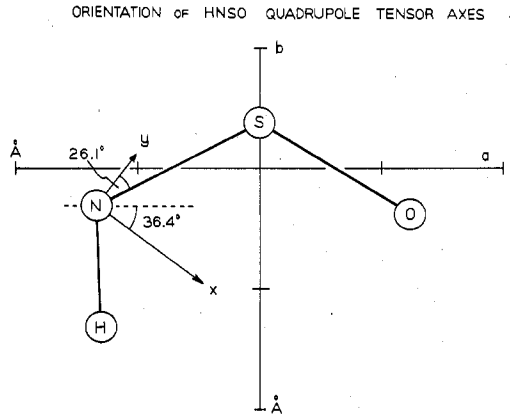

Figure 2. Projection of HNSO in symmetry plane showing principal inertial axes (a, b frame) and principal field gradient axes (x, y frame) of the nitrogen nucleus.

in χ_{aa} and η. A knowledge of these χ's and the angles of rotation between the substituted and parent principal inertial axes permits a determination of the field gradients (χ_{xx}, χ_{yy}, χ_{zz}) along the principal axes of the quadrupole tensor. For molecules with one isotopic substitution in a plane of symmetry, eq 9.115–9.121 in ref 7 are applicable if the structure is known. These were used to determine the quadrupole principal axes field gradients for $HNSOF_2$ and HNSO using the available data. The results are listed in Table II. Figures 1 and 2 illustrate the relative orientations of the inertial and field gradient principal axes systems in the symmetry plane; the orientation was chosen where $\chi_{cc} = \chi_{zz}$.

The determination of χ_{xx}, χ_{yy}, χ_{zz} for $HNSOF_2$ is dependent on only one coupling constant from $DNSOF_2$. Consequently, by using the reasonably accurate χ_{aa} for $DNSOF_2$, fairly precise values for them and the orientation angle can be obtained. The larger uncertainties for the HNSO species arise from the much smaller inertial rotation angle upon deuteration (~2.5°) leading to smaller changes in the observed χ_{aa}'s.

Table III. Ab Initio MO Results

	$HNSOF_2$			HNSO		
	r/Å	Mulliken overlap pop.	E_{AB}[a]	r/Å	Mulliken overlap pop.	E_{AB}
S–N	1.466	1.152	−1.948	1.512	0.797	−1.102
S–O	1.420	1.108	−1.941	1.451	0.744	−1.103
S–F	1.549	0.473	−1.076			
N–H	1.023	0.636	−0.840	1.029	0.603	−0.790
H···F		0.0004	−0.009			
H···O		0.0025	+0.017		0.003	−0.005

[a] Two-center contribution to the total energy; see text for definition; units are au. The calculated total energies were the following: $HNSOF_2$, −725.91207 au; HNSO, −527.08513.[20]

Table IV. Valence Orbital Populations and Net Charges

		$HNSOF_2$	HNSO			$HNSOF_2$	HNSO
S	3s	1.14	1.82	N	2s	1.63	1.66
	3p x[a]	0.93	0.88		2p x	1.25	1.31
	y	1.05	1.27		y	1.09	1.23
	z	0.90	0.98		z	1.58	1.29
	3d z^2	0.11	0.04		Q(net)	−0.54	−0.48
	xz	0.24	0.13				
	yz	0.18	0.02	F	2s	1.93	
	x^2-y^2	0.20	0.14		2p x	1.73	
	xy	0.22	0.14		y	1.90	
	Q[b](net)	1.02	0.57		z	1.66	
O	2s	1.82	1.83		Q(net)	−0.24	
	2p x	1.71	1.33	H		0.66	0.67
	y	1.12	1.68		Q(net)	0.34	0.33
	z	1.69	1.58				
	Q(net)	−0.34	−0.42				

[a] z axis is perpendicular to symmetry plane; y axis is oriented along the NS bond in both compounds. [b] Q(net) = valence electrons (free atom) − orbital populations.

The uncertainties in the experimental χ's and their propagation into the principal quadrupole tensor components are also sufficient to cover a 1–2% change in the experimental χ's upon deuteration due to a vibrational effect. Changes of about 1% are clearly seen in CH_3X, X = Cl, Br, I, upon deuteration;[8] similar shifts are also indicated upon deuteration in some nitrogen compounds although the small coupling constant for ^{14}N makes identification tenuous in some cases. The absolute magnitude of the effect for ^{14}N coupling constants falls between 0.1% for eQq_a in ND_3[9] and about 2% for eQq_c in *cis*-DONO[10] and *trans*-DONO[10] and for eQq_a in NF_2D.[11]

MO Calculation. All electron ab initio MO–SCF calculations were carried out by using the IBMOL-6 computational scheme[12] with Gaussian type orbitals contracted in a double-ζ form (9/5 to 4/2) as described by Snyder and Basch.[13] d polarization functions were added to the basis set of the sulfur atom but not to the basis set of the fluorine atom. The experimental structures for HNSO[4] and $HNSOF_2$[5] were employed.

Atomic and overlap populations were computed using Mulliken's definitions.[14] The bond energy analysis was performed following Clementi's procedure for the partitioning of the total energy in multicenter terms.[15] One-electron properties (dipole moment and electric field gradient) were computed by using the "Expectation Values Over Molecular Gaussian Wave Functions" written by Kortzeborn.[16] Results of these calculations are summarized in Tables II–IV.

Analysis and Discussion

Overlap Populations. Table III contains a summary of the bond lengths, the Mulliken overlap populations, and the two-center contributions to the total energy, E_{AB}.[15] The latter are a measure of bonding ($E_{AB} < 0$), or nonbonding ($E_{AB} > 0$), atom interactions.

The most significant change is the strengthening of the SN and SO bonds in $HNSOF_2$ relative to HNSO in both computed indicators. Some increase was perhaps expected because of the shorter bonds in $HNSOF_2$; however, the large magnitude of the change is a reflection of significant electronic interaction. Also of interest are the small H···O bonding interaction in HNSO and the slightly larger H···F bonding interaction in $HNSOF_2$. In the latter molecule the H···O interaction is nonbonding. Employing these E_{AB} terms, the hydrogen atom is stabilized in the cis configuration of HNSO by about 3 kcal but in $HNSOF_2$ it prefers the trans configuration with an interaction energy of about 11 kcal with the two fluorine atoms. It is attractive, therefore, to account for the change in configuration from cis to trans as arising from a better interaction of H when staggering two fluorines in $HNSOF_2$ compared to eclipsing the oxygen.

Orbital Populations. Table IV lists the atomic orbital populations as well as the net charges. It is observed that upon adding two fluorines to HNSO, the hydrogen charge is hardly altered while sulfur and oxygen lose electronic charge. This is consistent with the very high electronegativity of fluorine. However, the nitrogen atom gains electron charge. The nitrogen charge is contrary to simple intuition but insight is provided by examining the individual orbitals on N and S. The nitrogen p_x and p_y orbitals in the symmetry plane of $HNSOF_2$ have lost electron charge (σ transfer through the sulfur due to the very electronegative fluorines) but this has been compensated by a larger gain in the $p_\pi = p_z$ orbital. Sulfur orbitals interact with atoms other than nitrogen but it is noted that the p_z orbital population decreases only slightly while all the d orbital populations increase. These increases in π charge densities at N and S are consistent with the observed shortening of the NS bond in $HNSOF_2$ and with the increase of the NS overlap population and the E_{NS} contribution and are supportive of increased π-bond character between N and S.

Quadrupole Coupling Constants. The computed and observed nuclear quadrupole coupling constants are listed in Table II. These are proportional to the field gradients in the principal axes of the quadrupole tensor by the relationships $\chi_{xx}(\mathrm{MHz}) = eQ(\delta^2V/\delta x^2)$, etc. ..., where e is the electronic charge and Q is the nuclear electric quadrupole moment of nitrogen. A value of $Q = 0.156 \times 10^{-24}$ cm^2 [17] was used.

The agreement between relative signs, magnitudes, and orientation of the quadrupole tensor in the molecular axes is very satisfactory, lends credibility to the MO electron densities, and provides insight into the origin of the large differences between HNSO and $HNSOF_2$. The change in sign for the out-of-plane coupling constant, χ_{zz}, is principally associated with the significantly higher orbital occupation of the $p_z = p_\pi$ orbital relative to the in-plane p_x, p_y orbitals in going to $HNSOF_2$. These changes in orbital occupations are great enough to alter the relative distribution of p-electron density about the nitrogen nucleus. This significantly alters the orientation and interaction energy of the nitrogen nuclear quadrupole moment in the two molecules.

This interpretation for the out-of-plane coupling constant is qualitatively similar to that obtained by application of the simple formula discussed by Gordy and Cook[7]

$$\chi_{zz} = -(U_p)_z eqQ_{N10} \quad (1)$$

In this case χ_{zz} is the out-of-plane coupling constant and eQq_{N10} is the coupling constant due to one electron in a p orbital. For nitrogen, eqQ_{210} is taken as −10 MHz.[7] $(U_p)_z$ represents the unbalanced p electrons in the z direction

$$(U_p)_z = (n_x + n_y)/2 - n_z \quad (2)$$

and a positive $(U_p)_z$ corresponds to a p electron deficit in the z direction and vice versa. Table V illustrates the values for $(U_p)_z$ calculated from the experimental coupling constants and the calculated coupling constants (eq 1) and from the ab initio orbital populations (eq 2). It is seen that $HNSOF_2$ has an electron excess out of the plane compared to HNSO and this confirms our previous finding of increased π bonding in the former molecule. Since the experimental and computed χ_{zz} coupling constants are very close, the corresponding $(U_p)_z$ values in Table V obtained using eq 1 are obviously in good agreement. The agreement using the ab initio orbital populations is not very good, but the qualitative change between HNSO and $HNSOF_2$ is nevertheless reflected. This shows that the approximate method of Townes and Dailey,[18] and extended by Gordy,[19] for the interpretation of quadrupole coupling constants (in which eq 1 and 2 find their origin) can be employed with confidence for giving trends or qualitative changes but should be used with care for estimating accurate orbital populations.

Table V. Unbalanced p Electrons in Out-of-Plane Direction, $(U_p)_z$, Estimated by Different Methods

$(U_p)_z$[a]	HNSO	$HNSOF_2$
From exptl χ_{zz}	0.16	−0.22
From ab initio χ_{zz}	0.15	−0.26
From ab initio orbital pop.	−0.02	−0.41

[a] See text for relationship between U_p, coupling constants, and orbital populations.

One of the more striking comparisons is the good agreement obtained for the orientation of the quadrupole tensor axes between MO calculation and experiment. The experimental determination of this orientation is usually difficult and it often is necessary to interpret experimental quadrupole coupling constants from microwave spectroscopy. It appears that MO theory may be used to obtain a fairly reliable estimate for this orientation.

Dipole Moment Components. In the previous study[5] it was shown that the total dipole moment is oriented approximately parallel to the SO bond in $HNSOF_2$ with the negative direction toward the fluorines. The experimental values are $|\mu_a| = 0.65$ D, $|\mu_b| = 2.34$ D, and $\mu_T = 2.43$ D. The ab initio calculations also support this. It gave $\mu_a = 0.95$ D, $\mu_b = -3.25$ D, and $\mu_T = 3.38$ D and an orientation within 1° of the experimental finding. (Consult Figure 2 in ref 5 for orientation and signs.) The dipole orientation is more reliably estimated than the magnitude; this is due to the lack of polarization functions in the basis set of the fluorine atom.

For HNSO, good agreement between theory and experiment is obtained for both magnitude and orientation: experimental, $|\mu_a| = 0.89$ D, $|\mu_b| = 0.19$ D, $\mu_T = 0.91$ D; ab initio $\mu_a = -0.94$ D, $\mu_b = -0.03$ D, $\mu_T = 0.94$ D. (The dipole moment lies approximately along the a inertial axis with negative end toward nitrogen.)

From a cursory inspection of the charges in Table IV, a simple rationalization for the large difference in the dipole moments of the two compounds is not apparent. One may speculate on the basis of individual bond moments about the interpretation of the magnitude and orientation of the dipole moment in both molecules. Nevertheless, the large increase and the rotation of the dipole moment from approximately the S–N bond direction toward the S–F bonds when going from HNSO to $HNSOF_2$ can be readily attributed to a predominant contribution of the SF bonds.

Acknowledgment. This work was supported by the NATO Scientific Affairs Division (Research Grant No. 925) and by a grant to the University of Michigan from the National Science Foundation (CHE 76-09572).

Registry No. $DNSOF_2$, 63848-86-2; $HNSOF_2$, 20994-96-1; *cis*-HNSO, 40908-38-1.

References and Notes

(1) (a) Laboratoire de Chimie de Coordination. (b) University of Michigan.
(2) Both HNSO and $HNSOF_2$ have a symmetry plane containing the HNSO group. The cis/trans designation indicates the orientation of hydrogen relative to oxygen. A *trans*-HNSO isomer has also been observed at low temperatures in a matrix.[3] Only the trans isomer of $HNSOF_2$ is known.
(3) P. O. Tchir and R. D. Spratley, *Can. J. Chem.*, **53**, 2331 (1975).
(4) W. H. Kirchhoff, *J. Am. Chem. Soc.*, **91**, 2437 (1969).
(5) P. Cassoux, R. L. Kuczkowski, and R. A. Creswell, *Inorg. Chem.*, **16**, 2959 (1977).
(6) C. H. Townes and A. L. Schawlow, "Microwave Spectroscopy", McGraw-Hill, New York, N.Y., 1955, Chapter 6.
(7) W. Gordy and R. L. Cook, "Microwave Molecular Spectra", Interscience, New York, N.Y., 1970.
(8) J. W. Simmons and J. H. Goldstein, *J. Chem. Phys.*, **20**, 122 (1952).
(9) G. Herman, *J. Chem. Phys.*, **20**, 875 (1958).
(10) A. P. Cox, A. Brittain, and D. J. Finnegan, *Trans. Faraday Soc.*, **67**, 2179 (1971).
(11) D. R. Lide, *J. Chem. Phys.*, **38**, 456 (1963).
(12) E. Clementi, G. Lie, R. Pavani, and L. Gianolio, IBMOL-6 Program, Technical Report DDC-771, Mondedison S.p.A. (1977); E. Clementi, personal communication.
(13) L. C. Synder and H. Basch, "Molecular Wave Functions and Properties", Wiley, New York, N.Y., 1972.
(14) R. S. Mulliken, *J. Chem. Phys.*, **23**, 1833 (1955).
(15) E. Clementi, *Int. J. Quantum Chem.*, **3**, 179 (1969).
(16) R. N. Kortzeborn, "Expectation Values Over Molecular Gaussian Wave Functions", Special IBM Technical Report, San Jose, Calif., 1969.
(17) C. T. O'Konski and T. K. Ha, *J. Chem. Phys.*, **49**, 5334 (1965).
(18) C. H. Townes and B. P. Dailey, *J. Chem. Phys.*, **23**, 118 (1955).
(19) W. Gordy, *Discuss. Faraday Soc.*, **19**, 9 (1955).
(20) A lower energy of −527.19441 au was reported[21] for another ab initio calculation on *cis*-HNSO employing a basis set of similar size. Differences in contraction of the basis are the probable origin for the small energy difference between the two calculations.
(21) B. Solouki, P. Rosmus, and H. Bock, *Angew. Chem., Int. Ed. Engl.*, **15**, 384 (1976).

Contribution from the Department of Chemistry, University of Illinois at Chicago Circle, Chicago, Illinois 60680

Nonisomorphic Antiferromagnetic Behavior of Two Isomorphic Salts: Low-Temperature Heat Capacities and Magnetic Susceptibilities of $(NH_4)_2FeCl_5 \cdot H_2O$ and $K_2FeCl_5 \cdot H_2O$

J. N. McELEARNEY* and S. MERCHANT

Received August 12, 1977

The heat capacities and principal-axis magnetic susceptibilities at low temperatures are reported for single crystals of the isomorphic compounds $(NH_4)_2FeCl_5 \cdot H_2O$ and $K_2FeCl_5 \cdot H_2O$. The heat capacity of the diamagnetic isomorph $(NH_4)_2InCl_2 \cdot H_2O$ is also reported. Antiferromagnetic transitions are observed in both iron compounds. There are two in $(NH_4)_2FeCl_5 \cdot H_2O$: one at 6.87 ± 0.01 K and another at 7.25 ± 0.01 K; the single transition observed in $K_2FeCl_5 \cdot H_2O$ occurs at 14.06 ± 0.01 K. Spin canting is observed for $(NH_4)_2FeCl_5 \cdot H_2O$ but not for the potassium analogue. The indium compound has been used in a corresponding-states procedure to determine the magnetic heat capacities of the iron analogues. The results indicate the presence of a significant amount of lower dimensional exchange in $(NH_4)_2FeCl_5 \cdot H_2O$. However, although there is extensive exchange in $K_2FeCl_5 \cdot H_2O$, it is not lower dimensional in nature. The heat capacity and magnetic susceptibility data on $(NH_4)_2FeCl_5 \cdot H_2O$ have been analyzed using lower dimensional models, and an attempt has been made to interpret the differences in the behavior of the iron compounds in terms of the structures, which consist of $[FeCl_5(OH_2)]^{2-}$ and NH_4^+ groups. Hydrogen bonds and Cl–Cl contacts appear to be responsible for the observed exchange.

Introduction

One of the classical and most fruitful methods used to aid in understanding magnetic phenomena is the study of isomorphic materials. Through such studies important insights regarding the interplay of crystal field effects, spin magnitudes, spin dimensionalities, and structural characteristics have been gained. Such has been especially true in recent years regarding the study of lower dimensional compounds.[1] Many of the lower dimensional compounds which have been studied have been double salts of the form AMX_3 or A_2MX_4, where A is an alkali ion or a substituted ammonium group and X is a halide. Some 1:1 hydrated double salts have also been shown to be lower dimensional.[2-7] Usually the 2:1 hydrated salts consist of isolated monomeric species which display interesting, albeit three-dimensional, magnetic characteristics in the 1–4 K region.[8-17] In the case of $Rb_2NiCl_4 \cdot 2H_2O$,[18] however, the presence of hydrogen bonds in the material gave rise to lower dimensional behavior. All of the studies of the magnetic properties of the 2:1 hydrated compounds have involved divalent ions of the first-row transition metals—no such studies on the most stable trivalent species, Fe(III), have been made before. In fact, as a review[19] has recently pointed out, the coordination chemistry of Fe(III) has been neglected until recently.

Thus, since Fe(III) salts, containing high-spin S-state ions, are expected to be good models of Heisenberg systems and since such systems (usually Mn(II) salts) have attracted wide attention in lower dimensional magnetic studies, the first magnetic studies on hydrated double salts of Fe(III) have been made and are reported here. As it turns out, there are many such compounds, all having the general formula $A_2FeX_5 \cdot H_2O$, where A can be K, NH_4, Rb, Cs, or Tl and X can be F, Cl, or Br. In addition, In(III) analogues of the compounds also exist. The attractiveness of this series should be evident since it presents the possibility of studying the effects of relatively small structural variations on magnetic properties. The availability of a diamagnetic isomorph is also quite useful. The studies discussed here involve low-temperature single-crystal magnetic susceptibility and heat capacity measurements of $(NH_4)_2FeCl_5 \cdot H_2O$, $K_2FeCl_5 \cdot H_2O$, and $(NH_4)_2InCl_5 \cdot H_2O$. The ammonium and potassium members of the series were chosen for the initial work since those ions are typically of comparable size and the compounds would therefore be expected to exhibit

* To whom correspondence should be addressed at 1618 North Central Avenue, Chicago, Ill. 60639.

0020-1669/78/1317-1207$01.00/0